Steel and Composite Structures, *Vol. 34, No. 3 (2020) 333-345*
DOI: https://doi.org/10.12989/scs.2020.34.3.333

Efficient cross-sectional profiling of built up CFS beams for improved flexural performance

M. Adil Dar[1], N. Subramanian[2], Mir Atif[3], A.R. Dar*[3], M. Anbarasu[4] and James B.P. Lim[5]

[1]Department of Civil Engineering, Indian Institute of Technology Delhi, New Delhi, India
[2]Consulting Engineer, Maryland, USA
[3]Department of Civil Engineering, National Institute of Technology Srinagar, J&K, India
[4]Department of Civil Engineering, Government College of Engineering Salem, Tamilnadu, India
[5]Department of Civil & Environmental Engineering, University of Auckland, New Zealand

(*Received March 28, 2019, Revised October 25, 2019, Accepted December 20, 2019*)

Abstract. In the past, many efficient profiles have been developed for cold-formed steel (CFS) members by judicious intermediate stiffening of the cross-sections, and they have shown improved structural performance over conventional CFS sections. Most of this research work was based on numerical modelling, thus lacking any experimental evidence of the efficiency of these sections. To fulfill this requirement, experimental studies were conducted in this study, on efficient intermediately stiffened CFS sections in flexure, which will result in easy and simple fabrication. Two series of built-up sections, open sections (OS) and box sections (BS), were fabricated and tested under four-point loading with same cross-sectional area. Test strengths, modes of failure, deformed shapes, load vs. mid-span displacements and geometric imperfections were measured and reported. The design strengths were quantified using North American Standards and Indian Standards for cold-formed steel structures. This study confirmed that efficient profiling of CFS sections can improve both the strength and stiffness performance by up to 90%. Closed sections showed better strength performance whereas open sections showed better stiffness performance.

Keywords: cold-formed steel; efficient profiling; experiment; flexural members; built-up section; buckling; strength

1. Introduction

Cold-formed steel (CFS) members are gaining popularity, primarily due to the numerous advantages offered by them over conventional hot-rolled steel members. However, CFS sections are different from hot-rolled steel sections in structural behaviour due to their thin-walled and slender profiles (Yu and Schafer 2006). Due to thin-walled nature of CFS sections, they are susceptible to various modes of buckling instabilities like local buckling, distortional buckling, etc. In the case of hot rolled steel sections, buckling is prevented by controlling the width to thickness ratio of the specimens. Generally, the width to thickness ratio of individual components of CFS members is high, hence are prone to premature buckling at moderate compressive stress levels (much below the yield stress). The past research has tackled this issue effectively (Dar *et al.* 2019a-f). CFS built-up members comprising of unstiffened sections experience small wave formation (buckling instability) at the initial stages of loading (Dar *et al*. 2018a, 2019a). This problem can be tackled effectively either by developing innovative sectional profiles with intrinsic resistance against premature buckling and/or by appropriate stiffening arrangement at vulnerable locations (Dar *et al.* 2018b, 2019b). The capacity of CFS sections can be made to reach up to their plastic moment through proper designing and detailing (Kumar and Sahoo 2016). In the past decade, due to advances in manufacturing technology, even complex cross-sections could be manufactured (Hancock 2016).

Considerable research has been carried out on the development of CFS sections with sectional profiles capable of developing resistance against premature buckling (Yu *et al*. 2018, Sudhir Sastry *et al*. 2015, Obst *et al.* 2016, Ye *et al*. 2018, 2016, Trahair and Papangelis 2018, Dar *et al.* 2015a, Manikandan *et al.* 2014, Wang and Young 2014, Paczos and Wasilewicz 2009, Schafer 2011, Grenda and Paczos 2019, Magnucki and Paczos 2009, Magnucki *et al*. 2010) as shown in Fig. 1. Most of this research work was carried out on cross-sections comprising of a single section only, resulting in mono-symmetric sections. Moreover, much of this research was based on numerical studies. Hence, the experimental validation of the efficiency of these sections was lacking. In addition, there was limited research on closed built-up sections that perform well, particularly due to their inherent resistance towards torsional buckling (Li *et al*. 2016, Laim *et al.* 2013). Hence this experimental research was taken up on closed built-up CFS sections also.

A few of the efficient cross-sectional profiles, which are achieved by judicious incorporation of intermediate stiffeners, are simple and easy to fabricate, and considered in this research are shown in Fig. 2. The development of efficient sections was carried out in a sequential manner so

*Corresponding author, Professor
E-mail: abdulrashid@nitsri.net

ISSN: 1229-9367 (Print), 1598-6233 (Online)

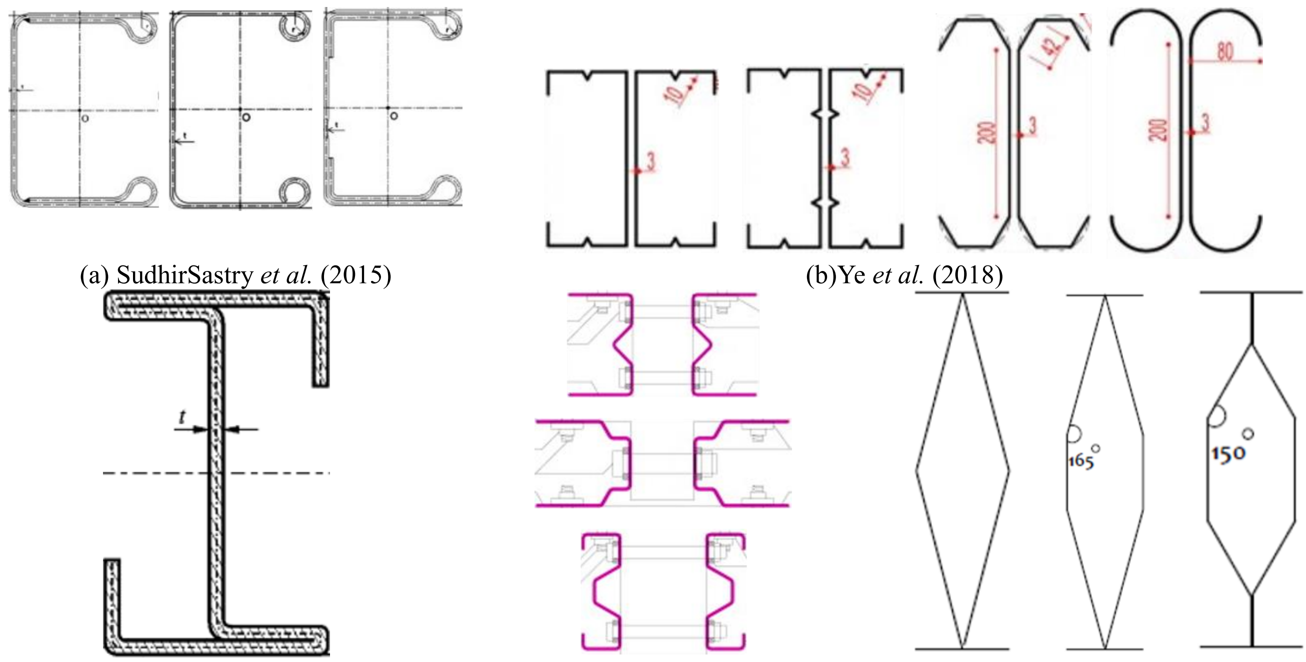

(a) SudhirSastry *et al.* (2015) (b)Ye *et al.* (2018)

(c) Paczos and Wasilewicz (2009) (d) Wang and Young (2014) (e) Dar *et al*. (2015a)

Fig. 1 Improved cross-sectional profiles developed in the past

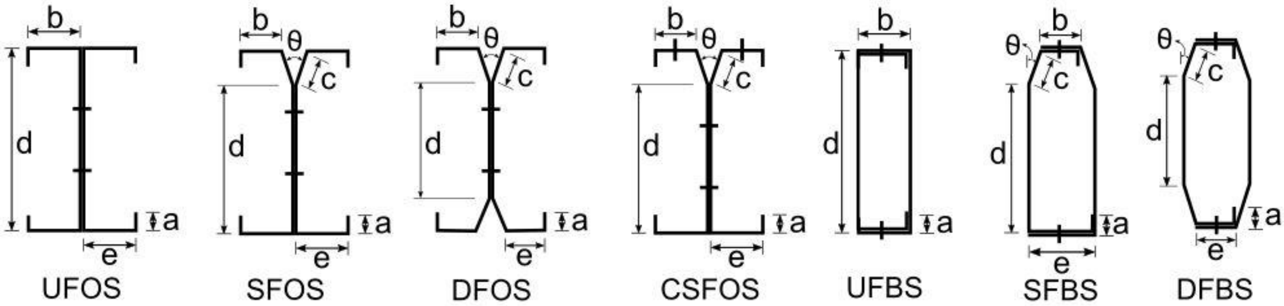

Fig. 2 Cross-sectional details of models

that improved flexural performance of CFS beams is achieved, with better material utility and economy. The intermediate stiffeners were incorporated by using simple press braking without the need for cold-rolling machines. This type of testing on such sequential intermediate stiffening of CFS beams has been attempted for the first time. These test results will be invaluable to check the results of numerical modelling of such sections and may aid extensive parametric studies. As stated earlier, the efficiency of this sequential intermediate stiffening was evaluated for both open as well as closed CFS built-up beams as shown in Fig. 2.

The present investigation aims at sequential efficient profiling of built-up CFS open and box sections subjected to flexure. The CFS sections studied had the same cross-sectional area, but different shapes. Cross-sectional shape modifications were made progressively in each sample on the basis of preceding test results. The ultimate load carrying capacity, failure modes, deformed shapes, load vs. mid-span displacements and geometric imperfections were measured and reported. The experimental results of the beam models are also compared with the design strength predicted by North American Specifications and Indian Standard for cold-formed steel structures.

2. Experimental Investigation

To study the effect of efficient cross-sectional profiling on the flexural behaviour of CFS beams, seven specimens were fabricated. Mild steel sheets of 1.6 mm thickness were used for fabrication of all the test specimens. The total length of the specimens was 2.3 m with an effective length of 2.1 m between supports. To form open sections, four specimens were fabricated by connecting two channel sections back to back with two rows of self-drilling screws (SDS) of 6.4 mm diameter at middle third points along the depth of the members and spaced at 200 mm centre-to-centre longitudinally. To form box sections, three specimens were fabricated by connecting two channel sections toe-to-

Table 1 Nominal and measured dimensions of specimens

Specimen	Nominal (mm)						Measured (mm)					
	a	b	c	d	e	θ	a	b	c	d	e	θ
UFOS	20	70	-	220	70	-	20.3	69.4	-	221.1	70.2	-
SFOS	20	60	55	165	80	40	20.2	61.3	55.1	166.3	80.7	37
DFOS	20	60	55	130	60	40	19.6	60.2	55	128.4	59.2	38
CSFOS	20	60	55	165	80	40	20	60.6	55.3	164.1	79.3	37
UFBS	20	70	-	220	70	-	20.5	70.7	55.2	222.1	68.8	-
SFBS	20	60	55	165	80	40	21.3	59.2	55.4	164.8	78.6	22
DFBS	20	60	55	130	60	40	19.7	59.6	54.6	131.6	61.4	23

toe at flanges as shown in Fig. 2. A single row of SDS was used to join the sections at both top and bottom flange levels with a uniform spacing of 200mm along the length of the member. The dimensional details of all the specimens are given in Table 1. The cross-sectional dimensions were measured using a digital vernier calliper.

2.1 Justification for choosing the proposed cross-sections

2.1.1 Specimen 1: UFOS

This most common built-up section used and is formed by connecting two channel sections back-to-back as shown in Fig. 2. Such an open section (OS) is conventionally used in CFS construction. This specimen was fabricated to serve as a benchmark model for the purpose of comparison of the other improved built-up sections. This specimen will help in the quantification of the improvement in flexural performance of other efficient specimens in the OS series.

2.1.2 Specimen 2: SFOS

To reduce the unsupported width of slender elements in compression, a fold (intermediate stiffener) was introduced in the compression part between the web and the flange of a lipped channel. This would increase the effective area of the cross-section for improved flexural performance. Two such lipped channels with a single fold in the compression zone were joined back to back to form this specimen as shown in Fig. 2.

2.1.3 Specimen 3: DFOS

To study the effect of intermediate stiffener in the tension zone, a further modification was made in SFOS by introducing a similar fold (intermediate stiffener) between web and tension flange of the section. This would impart the necessary symmetry to the cross-section. One of the intermediate stiffeners was provided in compression whereas the other was provided below neutral axis in the tension part of web. These folded sections were joined back to back as shown in Fig. 2.

2.1.4 Specimen 4: CSFOS

To further improve the performance of SFOS by arresting/delaying the instability failure, this specimen was fabricated by adding a U shaped cap over the compression flange of SFOS. The thickness of the compression flange was effectively doubled while it acted as a restraint to prevent outward movement of the compression flanges, especially at load points as seen in SFOS. The shear connection between cap and flange was provided by drilling two rows of screws at a uniform spacing of 200mm in the longitudinal direction. The geometry of the cross-section is shown in Fig. 2.

2.1.5 Specimen 5: UFBS

Since closed sections perform better than OS in terms of their torsional rigidity, a BS was fabricated by connecting a lipped channel with an un-lipped channel to form a box type built-up section as shown in Fig. 2. This model was fabricated to serve as a benchmark for evaluating the improved performance of other efficient BS sections.

2.1.6 Specimen 6: SFBS

To reduce the unsupported width of slender elements in compression, a single fold was introduced in the compression part of the specimen between the web and the flange as shown in Fig .2 (similar to SFOS). Such an introduction of an additional stiffener would improve the structural performance of the modified cross-section.

2.1.7 Specimen 7: DFBS

A modification similar to DFOS was made in UFBS by adding another intermediate stiffener between the web and the flange of the individual elements of the section in the tension zone. Here, both the lipped channel and un-lipped channel had two folds at either junction between the web and flange of the elements. The webs for box sections are slender as compared to the open sections, as they are not connected back to back as shown in Fig. 2. Further, the provision of folds on either connection between webs and flanges imparted symmetry to the cross-section.

2.2 Numerical simulation procedure

2.2 1 Material properties:

Mild steel sheets (1.6 mm) conforming to Indian Standard IS-2062, available locally, were used in this study. The grade designation of the sheets was E250 with quality designated as A. Tensile coupon tests were carried out in accordance with IS-1608 (2005), which prescribes the

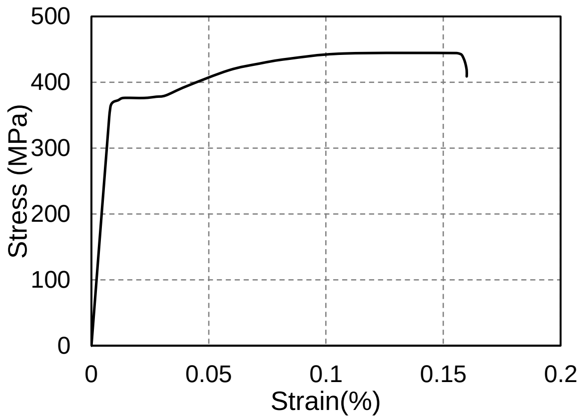

Fig. 3 Stress vs. strain curve of CFS used

Table 2 Material properties of the steel used

S. No	E (GPa)	F_y (MPa)	F_u (MPa)	δ (%)
1	209	372.30	422.37	18
2	207	361.16	414.75	20
3	208	377.08	417.93	23
4	212	369.01	447.74	19
5	210	360.21	425.37	25
Average	*209*	*367.95*	*425.64*	*21*

Table 3 Imperfections measured in the specimens

Model	UFOS	SFOS	DFOS	CSFOS	UFBS	SFBS	DFBS
δ_1/L	1/3443	1/2625	1/4167	1/3152	1/3847	1/4423	1/3526
δ_2/L	1/3763	1/2932	1/3652	1/3282	1/3526	1/3973	1/3681

method of conducting tensile test on a steel sheet strip of thickness less than 3 mm and greater than 0.5 mm, to determine the mechanical properties of material used. Coupons were fabricated from the flanges of the test specimens near their mid-span, in the longitudinal direction of the sheet. A total of five coupon tests were conducted in the study and their results are given in Table 2. Typical stress vs. stress plot of coupon tests is shown in Fig. 3.

2.3 Geometrical imperfections

After the fabrication of specimens, the initial overall geometric imperfections were recorded. The imperfections were determined at the bottom flange to web junctions near the centre along both the longitudinal and transverse directions. An optical theodolite and a calibrated digital vernier calliper were used to obtain the readings at the mid-span and near both ends of the test specimens. The imperfections measured at the mid-span along the specimen in the two orthogonal directions (Fig. 4) are given in Table3. Maximum geometric imperfection measured at the mid-span in δ1& δ2 direction was 1/2625and 1/2932 respectively and found in SFOS while minimum imperfection was observed for SFBS at the mid-span (1/4423, 1/3973). As a comparison, the magnitude of the maximum and minimum imperfections measured by (Dar *et al*. 2018) were 1/2167 and 1/4112 respectively.

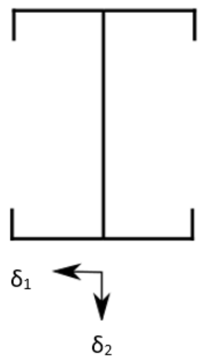

Fig. 4 Directions of imperfection measurement

Fig. 5 Specimen mounted on the test rig

2.4 Test setup

The specimens were mounted on a 200 kN capacity loading frame as shown in Fig. 5. They were subjected to four-point loads at the centre of the beam, to study the flexural behaviour and the test set-up is shown in Fig. 6. A 200 kN capacity hydraulic jack was used to apply the load, which was transferred to the test specimen by means of a rigid load spreader beam, composed of two-channel sections (ISMC 100×50) joined toe to toe. Digital dial gauges of least count 0.01 mm and 75 mm travel were used to record vertical deflection of specimens at mid-span and loading points. All the test specimens were laterally unrestrained and tested under simply supported end conditions with pinned support on one side and roller support on the other side. Bearing plates of size 200 mm × 100mm × 10mm were placed at loading points to prevent punching failure due to concentrated loads. Bearing stiffeners comprising of two angles (55 mm×45 mm×1.6 mm) connected back to back and made of the same material as the test specimen was used to prevent web buckling at points of concentrated loads. The other details pertaining to the test set-up can be found elsewhere (Dar *et al.* 2019c).

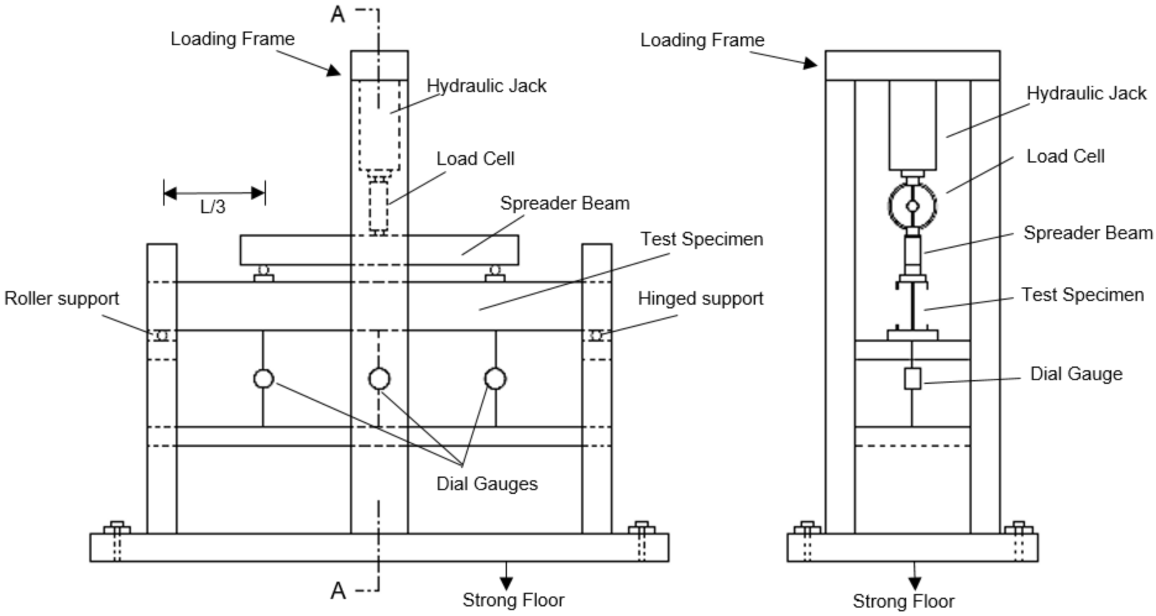

Fig. 6 Schematic view of loading arrangement

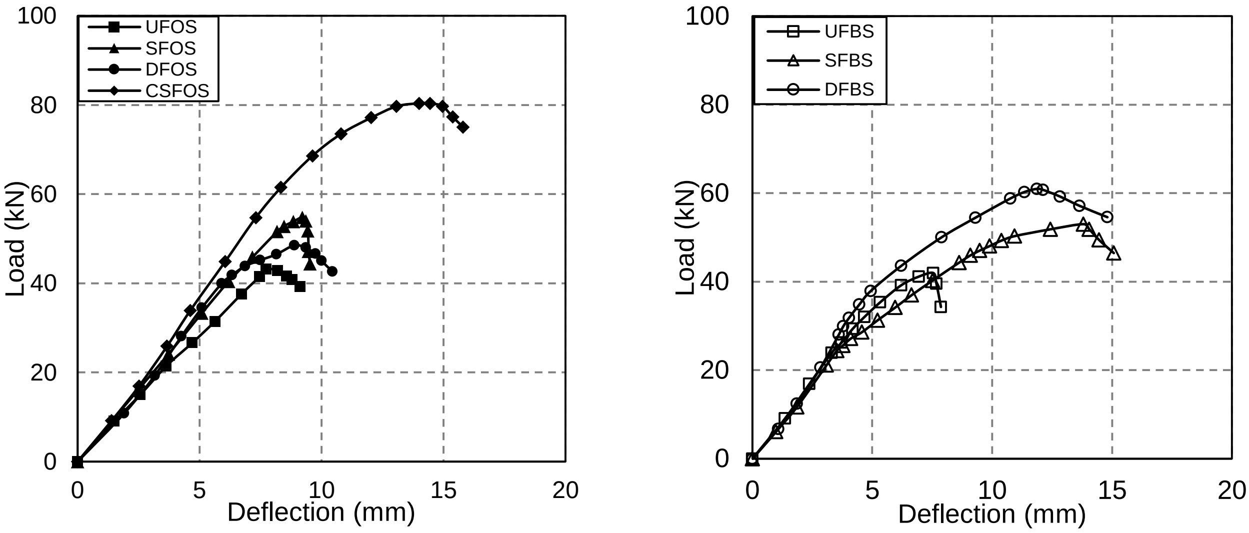

Fig. 7 Load vs. mid-span deflection curves for OS and BS series

3. Test results and discussions

Fig. 7 shows the load vs. mid-span deflection curves for OS and BS series specimens. The specimen UFOS failed primarily by flexural buckling. However, local buckling was observed under one of the loading points at a load of 39 kN, which was characterized by buckling of compression flange towards the web prior to out of plane deformation of edge stiffener and the beam web (as seen in Fig. 8). The half-wavelength of buckling measured across the loading point was 76 mm. Due to relatively shorter span, there was no lateral torsional buckling, as expected. Furthermore, insufficient screws in the bearing stiffener lead to its buckling (as seen in Fig. 8). The maximum load recorded was 42.78 kN and corresponding mid-span displacement was 7.75 mm

Since, SFOS was a modified version of UFOS (a fold, i.e., an intermediate stiffener) was introduced in the compression part between the web and the flange junction). The specimen SFOS failed due to the interaction of local buckling and lateral torsional buckling as shown in Fig. 9. The specimen failure was initiated by local buckling of the compression flange in the flexural zone near one of the load points as shown in Fig. 9. Here, due to punching of compression flange towards the web, there was local buckling of compression folds towards each other. As the failure deflection increased significantly, the beam went into the plastic zone. At higher loading, torsional buckling was also observed. The maximum load recorded was 54.36 kN and corresponding mid-span displacement was 9.18 mm.

A further modification to sectional profile of SFOS was made by introducing a similar fold (intermediate stiffener) between web and tension flange of the section. The specimen DFOS failed due to a combination of distortional buckling and lateral torsional buckling as shown in Fig. 10. Distortional buckling started at a load of around 30.12 kN and was characterized by outward rotation of bottom flange about the fold-flange line as shown in Fig. 10(b). As the load was further increased, this buckling became more evident and the half-wavelength stabilized at a load of 39.15 kN. The measured half wavelength of this buckling was 650 mm. With further increase in load, there was lateral movement of the specimen between supports coupled with local buckling of folds below one of the loading points. The maximum load observed was 48.25 kN and corresponding mid-span displacement was 10.04 mm.

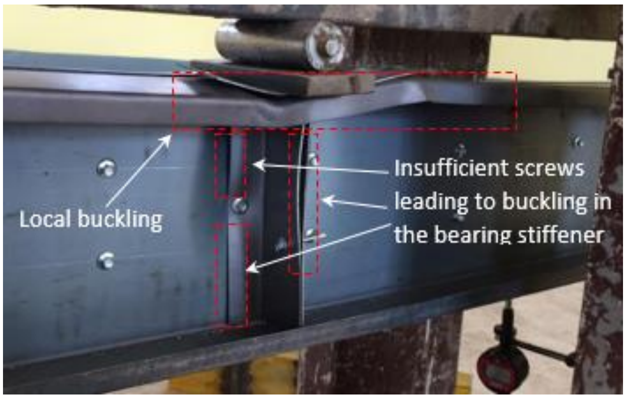

Fig. 8 Failure in UFOS

Fig. 9 Failure in SFOS

(a) Lateral torsional buckling

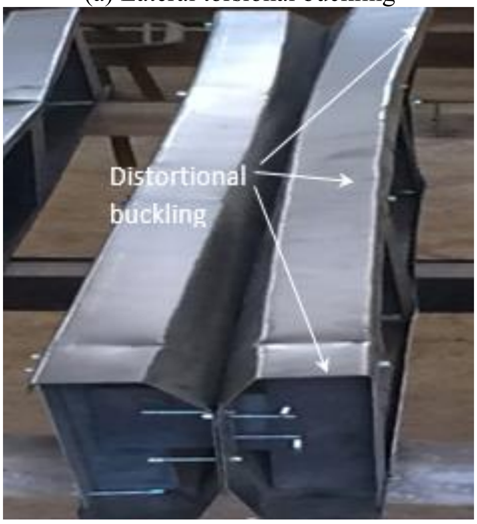

(b) Distortional buckling

Fig. 10 Failure in DFOS

A U-shaped cap was provided over the compression flange of SFOS sectional profile. The thickness of the compression flange was effectively doubled while it acted as a restraint to prevent outward movement of the compression flanges, especially at load points as seen in SFOS. This specimen carried a maximum load of 80.80 kN and a corresponding mid-span displacement of 14.2 mm. Due to addition of a U-shaped cap over the compression flange, local buckling was evidently delayed in the specimen. Compared to SFOS, local buckling of folds below loading points in the compression part was considerably less as shown in Fig. 11. Further, as the thickness of compression flange was effectively doubled (due to the provision of shear connection), the effective moment-resisting area in compression improved.

UFBS was fabricated to act as a reference for quantification of the improvement in the flexural performance of proposed efficient BS series. The beam failure was due to a combination of local buckling of compression flange as well as web in the pure moment zone as shown in Fig. 12. As the torsional strength of box section

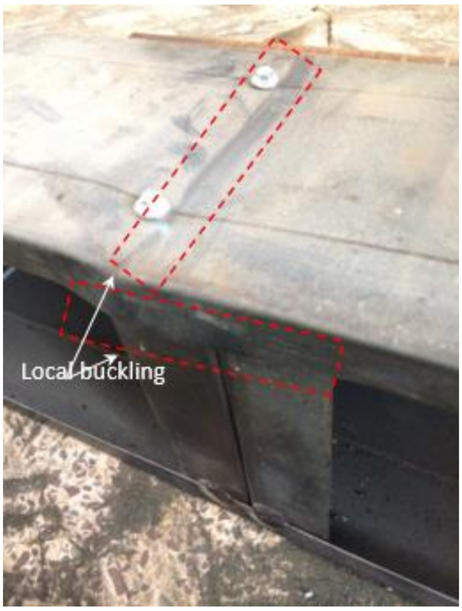

Fig. 11 Local buckling of CSFOS

Fig. 12 Web buckling of UFBS

is comparatively higher than that of open sections, lateral torsional buckling, as envisaged, did not occur. Failure of the specimen was a result of out of plane buckling of web above the neutral axis of specimen below one of the loading points as shown in Fig. 12. The maximum load recorded was 42.17 kN and corresponding mid-span displacement was 7.6 mm.

The UFBS profile was modified by incorporating a fold (intermediate stiffener) between the compression flange and the web of the section, resulting in a reduction of unsupported width of the web in compression and thus delayed its local buckling. The load vs. deflection curve and the behaviour of this modified specimen (SFBS) were similar to UFBS, albeit the buckling of web was delayed due to the presence of stiffening element in the web (fold). There was buckling of web above the neutral axis (as shown in Fig. 13) at a load of 42.78 kN. It should be noted that once the buckling of web started, with further increase of load, buckling concentrated at the intermediate stiffener in the web (on account of enhanced strength due to cold forming). The specimen finally failed due out of plane local buckling of web on both sides in the high moment zone. The measured half wavelength of buckling was 80 mm. The maximum load observed was 52.52 kN and corresponding mid-span displacement was 13.8 mm.

In order to further reduce the unsupported width of the webs, another fold (intermediate stiffener) was introduced to the sectional profile of SFBS. Further, the provision of folds on either connection between webs and flanges imparted symmetry to the cross-section. The maximum load observed was 61.03 kN and corresponding mid-span displacement was 12.88 mm. The failure of the specimen was primarily due to a combination of local buckling in the compression flange and compression part of the web [as shown in Fig. 14(a)] in the high moment zone (middle 700 mm length of the beam). During testing, part of specimen below the neutral axis showed a tendency to move outwards (at a load of 42.17 kN) as shown in Fig. 14(b). The same tendency was also seen in DFOS which ultimately led to distortional buckling of DFOS. In contrast, due to screw connection in flanges (as opposed to web in open sections), this tendency of the specimen was arrested. The beam ultimately failed due to combination of local buckling in flange and web in the high moment zone of the specimen. Local buckling in the flange could be seen throughout between the loading points (half wavelength of 100 mm) with buckling of web at the mid-span of the specimen on either side of cross-section.

In the case of open sections series of beams, the incorporation of intermediate stiffeners (folds) drastically improved the load-carrying capacity of the specimens. The improvement with reference to UFOS is quantified as 12.8%, 27% and 88.86% for DFOS, SFOS, and CSFOS, respectively (as shown in Fig. 15). It is worth mentioning that this improvement in load carrying capacity was achieved without any addition of material to the specimen, thus confirming the significant role of efficient profiling of CFS in resisting loads. Apart from this, in contrast to the expectations, the load carried by SFOS was more than that carried by DFOS. Basically, the provision of folds stirred out of plane movement of folded channel sections away from each other, particularly at loading points (folds above neutral axis) and supports (folds below neutral axis). This led to distortion of the cross-section and hence reduced the potential load-carrying capacity. Thus, for open sections, provision of single fold (in the compression flange) is better alternative than provision of two folds (both in compression and tension), unless adequate measures are taken to restrict lateral movement of flanges at points of load transfer. This concept was verified by the test results of CSFOS which led to 48.6% increase in load-carrying capacity when compared to SFOS. In addition, the stiffness improvement with reference to UFOS is quantified as 12.1%, 21.2% and 88.96% for SFOS, DFOS, and CSFOS, respectively (as shown in Fig. 16). The stiffness of the specimens was determined as the ratio of the ultimate moment to the corresponding rotation. The details of the procedure for determining the same can be found elsewhere (Dar *et al.* 2019c)

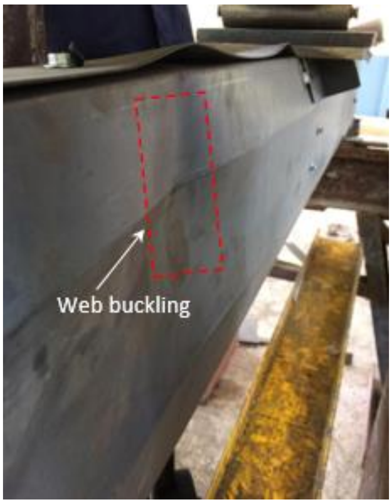

(a) Local buckling

(b) Distortion

Fig. 14 Failure in DFBS

Fig. 13 Web + flange buckling of SFBS

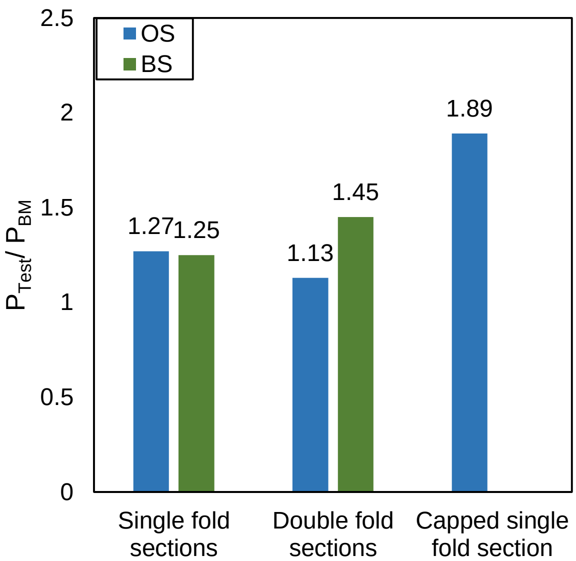

Fig. 15 Strength comparison in various specimens

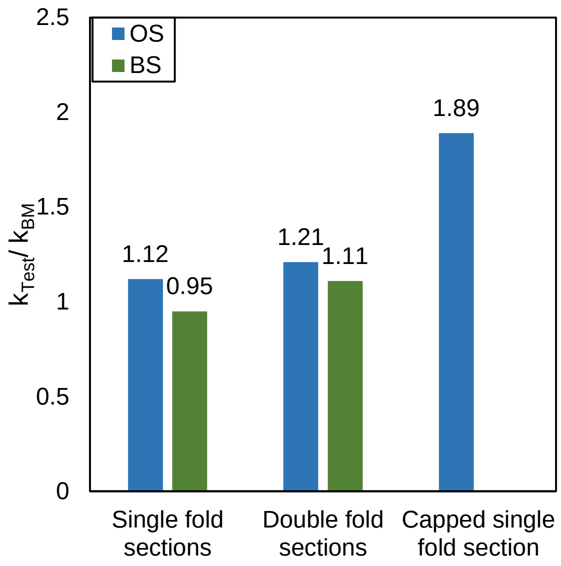

Fig. 16 Stiffness comparison in various specimens

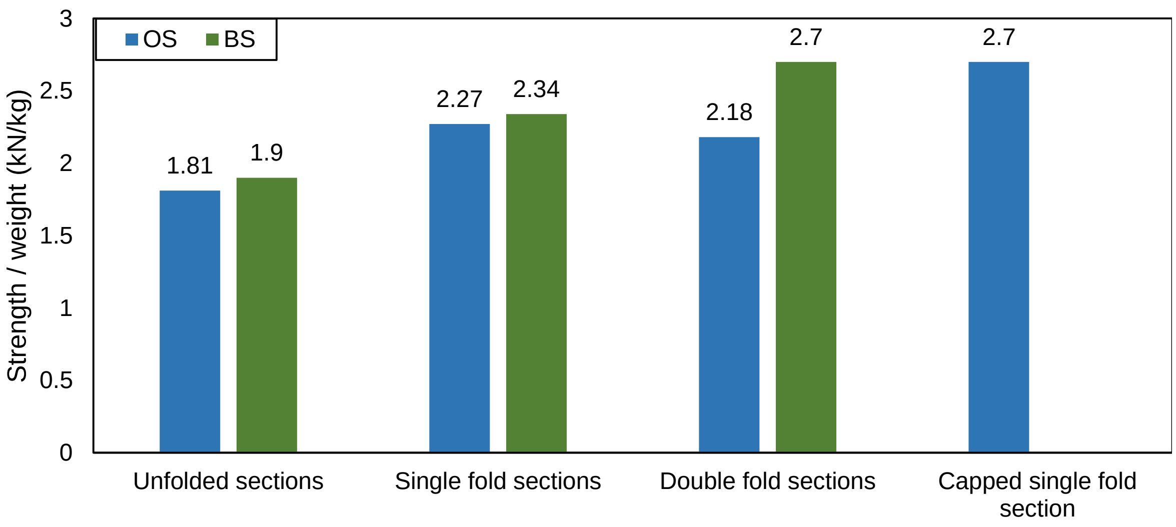

Fig. 17 Strength-to-weight ratio of test specimens

For box sections, the provision of folds (intermediate stiffeners) led to decrease in unsupported width of the slender webs and hence resulted in delayed local buckling, thereby increasing the built-up capacity of test specimens. In contrast to OS series, DFBS carried more load in comparison to SFBS. Although a similar phenomenon of outward movement of sections at loading points and supports was observed initially, the presence of connections (screws) in the flanges prevented this out of plane movement. The improvement with reference to UFBS is quantified as 24.5% and 44.7% for SFOS and DFOS, respectively. It was further observed that only DFBS showed improvement in stiffness with respect to UFBS (11%). In SFBS, there was a 5% drop in stiffness as compared to UFBS.

The strength to weight ratio of the specimens showed the same trend as shown by strength characteristics, except for DFBS as shown in Table 4 and Fig. 17.

Table 4 Strength-to-weight ratio of test specimens

Specimen	Strength (kN)	Weight (kg)	Strength / weight
UFOS	42.78	23.64	1.81
SFOS	54.36	23.93	2.27
DFOS	48.25	22.13	2.18
CSFOS	80.80	29.89	2.70
UFBS	42.17	22.24	1.9
SFBS	52.53	22.48	2.34
DFBS	61.03	22.57	2.70

In this study, the area of the cross-section was kept same within a given test series but the area varied between OS and BS series. Thus, direct comparison of load-carrying capacity of the two series will not provide true comparison. Moreover, the strength-to-weight ratio needs to be determined to compare the performance of open and box sections. The strength-to-weight ratio of the test specimens is given in Table 4. It can be observed from Figs. 8-11 that for OS series, CSFOS has the highest strength-to-weight ratio followed by SFOS, DFOS, and UFOS respectively. This confirms the observation made by Luis Liam *et al.* (2013) that use of two or more profiles increases the strength to weight ratio but the ratio doesn't increase when more than four profiles are used to form a built-up section. However, in comparison, box sections showed better strength-to-weight ratio than corresponding open sections of similar geometric configuration. In addition, box sections provide better aesthetics than open sections and hollow inside of the sections can be used to run service lines. Although this research focused only on pure flexural behaviour, it is well-established that box sections have higher torsional resistance than open sections. In view of all these observations, use of box beams is recommended over beams with open cross-sectional profiles.

4. Design rules

4.1 Design rules specified in AISI-S100-16 (DSM):

The procedure for calculating design strength of flexural members is summarised as follows:

Based on lateral torsional buckling:

- For doubly symmetric open section

$$F_{cre} = \frac{C_b * \pi^2 * E * d * I_{yc}}{S_f * (K_y * L_y)^2} \tag{1}$$

Where, F_{cre}= elastic buckling stress, C_b is a constant taken as unity conservatively, d = depth of section, I_{yc} = moment of inertia of compression portion of the section about centroidal axis of entire section parallel to web, using full unreduced section, E = modulus of elasticity of steel, K_y = effective length factor, L_y = unbraced length of member for bending about y axis

- For closed-box section members, if the laterally unbraced length of the member is less than or equal to Lu, the global buckling does not need to be considered, and the nominal stress, $F_n = F_y$.

$$L_u = \frac{0.36 * C_b * \pi}{F_y * S_f}\sqrt{E * G * J * I_y} \tag{2}$$

Where, J = Torsional constant of the closed-box section, I_y= Moment of inertia of full unreduced section about centroidal axis parallel to web, F_y = Yield stress

If the laterally unbraced length of a member is larger than L_u, the elastic buckling stress, F_{cre}, for bending about the symmetric axis shall be calculated as follow

$$F_{cre} = \frac{C_b * \pi}{K_y * L_y * S_f}\sqrt{E * G * J * I_y} \tag{3}$$

The nominal strength [resistance], M_{ne}, considering inelastic flexural reserve capacity is given by

For $M_{cre} > 2.78\ M_y$,

$$M_{ne} = M_p - (M_p - M_y)\frac{\sqrt{M_y/M_{cre}} - 0.23}{0.36} \tag{4}$$

For $2.78\ M_y > M_{cre} > 0.56\ M_y$,

$$M_{ne} = \frac{10}{9}M_y\left(1 - \frac{10\ M_y}{36\ M_{cre}}\right) \tag{5}$$

Where M_{cre} = Critical elastic lateral-torsional buckling moment, M_y = Member yield moment, M_p = Member plastic moment, Z_f = Plastic section modulus

Based on local buckling:

The local buckling moment, M_{crl}, of a member shall be based on the smallest buckling stress among elements in the cross-section, referenced to the extreme compression fibre, as follows

$$M_{crl} = S_f * F_{crl} \tag{6}$$

Where S_f= Gross elastic cross-sectional modulus referenced to the extreme compression fiber, F_{crl} = Local buckling stress at extreme compression fiber, given by

$$F_{crl} = K\ \frac{\pi^2 * E}{12\ (1 - \mu^2)}\left(\frac{t}{w}\right)^2 \tag{7}$$

Where, K = Plate buckling coefficient given in Appendix 1 of AISI S100-2016, E = Modulus of elasticity of steel, t = Element thickness, μ = Poisson's ratio of steel, w = Element flat width

The nominal flexural strength [resistance], M_{nl}, for considering the interaction of local buckling and global buckling shall be determined as follows

For $\lambda_l \le 0.776$

$$M_{nl} = M_{ne} \tag{8}$$

For $\lambda_l > 0.776$

$$M_{nl} = \left[1 - 0.15\left(\frac{M_{crl}}{M_{ne}}\right)^{0.4}\right]\left(\frac{M_{crl}}{M_{ne}}\right)^{0.4} M_{ne} \tag{9}$$

Where

$$\lambda_l = \sqrt{M_{ne}/M_{crl}} \tag{10}$$

M_{ne} = Nominal flexural strength [resistance] for lateral-torsional buckling, M_{crl} = Critical elastic local buckling moment

Based on distortional buckling:

The elastic distortional buckling moment, M_{crd}, shall be calculated as follows

$$M_{crd} = S_f * F_{crd} \tag{11}$$

Where

$$F_{crd} = \beta \frac{K_{\varphi fe} + K_{\varphi we} + K_{\varphi}}{K_{\varphi fg} + K_{\varphi wg}} \quad (12)$$

β is taken as unity conservatively; $K_{\phi fe}$ = elastic rotational stiffness provided by the flange to the flange/ web juncture, $K_{\phi we}$ = elastic rotational stiffness provided by the web to the flange/ web juncture, K_{ϕ} = Rotational stiffness provided by a restraining element (brace, panel, sheathing) to the flange/web juncture of a member (zero if the compression flange is unrestrained), $K_{\phi fg}$ = Geometric rotational stiffness demanded by flange from the flange/web juncture, $K_{\phi wg}$ = Geometric rotational stiffness demanded by the web from the flange/web juncture.

The nominal flexural strength [resistance], M_{nd}, shall be calculated as follows

For $\lambda_d \leq 0.673$

$$M_{nd} = M_y \quad (13)$$

For $\lambda_d > 0.673$

$$M_{nd} = \left[1 - 0.15 \left(\frac{M_{crd}}{M_y}\right)^{0.5}\right]\left(\frac{M_{crd}}{M_y}\right)^{0.5} M_y \quad (14)$$

Where

$$\lambda_d = \sqrt{M_y/M_{crd}} \quad (15)$$

$$M_y = S_{fy} * F_y \quad (16)$$

Where, S_{fy} = Elastic section modulus of full unreduced cross-section relative to extreme fibre in first yielding.

4.2 Design rules specified in IS-801

:

The code specifies the strength of flexural members as minimum obtained on the basis of yielding and lateral torsional buckling of the section-

Based on Yielding

Nominal Moment

$$M = 0.6 * f_y * Z_{xc} \quad (17)$$

Where, f_y = Specified minimum yield point, Z_{xc} = Elastic section modulus of effective section.

Based on Lateral Torsional Buckling

When, $\frac{0.36\ \pi^2\ E\ C_b}{F_y} < \frac{L^2\ Z_{xc}}{d\ I_{yc}} < \frac{1.8\ \pi^2\ E\ C_b}{F_y}$

$$f_b = \frac{2}{3} f_y - \frac{f_y^2}{5.4\pi^2 E C_b}\left(\frac{L^2 Z_{xc}}{d I_{yc}}\right) \quad (18)$$

When, $\frac{L^2 Z_{xc}}{d\ I_{yc}} \geq \frac{1.8\ \pi^2\ E\ C_b}{F_y}$

$$f_b = 0.6\ \pi^2\ E\ C_b \left(\frac{d\ I_{yc}}{L^2 Z_{xc}}\right) \quad (19)$$

Nominal Moment

$$M = f_b * Z_{xc} \quad (20)$$

Where, L = unbraced length of the member, Iyc = the moment of inertia of the compression portion of the section about the gravity axis of the entire section parallel to the web, Zxc = Compression section modulus of entire section about major axis, Ixx divided by distance to the extreme compression fiber, d = depth of the section, Cb = bending coefficient which can be conservatively taken as unity.

The other details pertaining to the determination of the design strengths of CFS beams using these standards can be found elsewhere (Dar *et al*. 2019c)

Table 5 and Fig. 18 shows the comparison of design strengths with the test results. The test results indicate that design predictions using IS801 are conservative as it still adopts working stress design methodology. Further, IS 801 does not account for check for distortional buckling, therefore, needs revision especially for closed sections subjected to flexure. The design strengths determined by AISI S100-16 overestimated load-carrying capacity of open CFS sections. The un-conservativeness in open sections may be due to their lesser torsional resistance when compared with the closed sections, in combination with possibility of mixed modes of buckling. Also, the interaction between the different elements of the built-up section is not considered in the design, which has been identified as one of the reasons that affect the behaviour of these built-up sections . Similar results (unconservative design strength prediction) were also observed in open sections studied by Luis *et al*. (2013), Manikandan *et al.* (2014). However, the AISI S100-16 underestimated the capacity of closed CFS sections, which may be primarily due to their larger torsional rigidity compared to the open sections. Furthermore, open sections are more susceptible to local and distortional buckling. It was concluded that method of joining the elements in a built-up section has a marked influence on the load-carrying capacity and as such, this provision should be incorporated in the design standards to predict the load-carrying capacity of built-up sections more accurately. Also, the high value of COV for the NAS (i.e., 0.24) would probably not allow these sections to be prequalified for the design according to the NAS.

Table 5 Design strength comparison with test results

Specimen	P_{Test}	P_{IS}	P_{NAS}	P_{Test}/P_{IS}	P_{Test}/P_{NAS}
UFOS	42.78	34.88	50.89	1.226	0.84
SFOS	54.36	34.81	59.91	1.562	0.9
DFOS	48.25	37.38	58.22	1.291	0.83
CSFOS	80.80	62.24	84.06	1.298	0.96
UFBS	42.17	33.48	37.09	1.296	1.14
SFBS	52.53	32.66	39.3	1.608	1.33
DFBS	61.03	34.99	42.11	1.744	1.45
Mean				*1.43*	*1.06*
COV				*0.20*	*0.24*

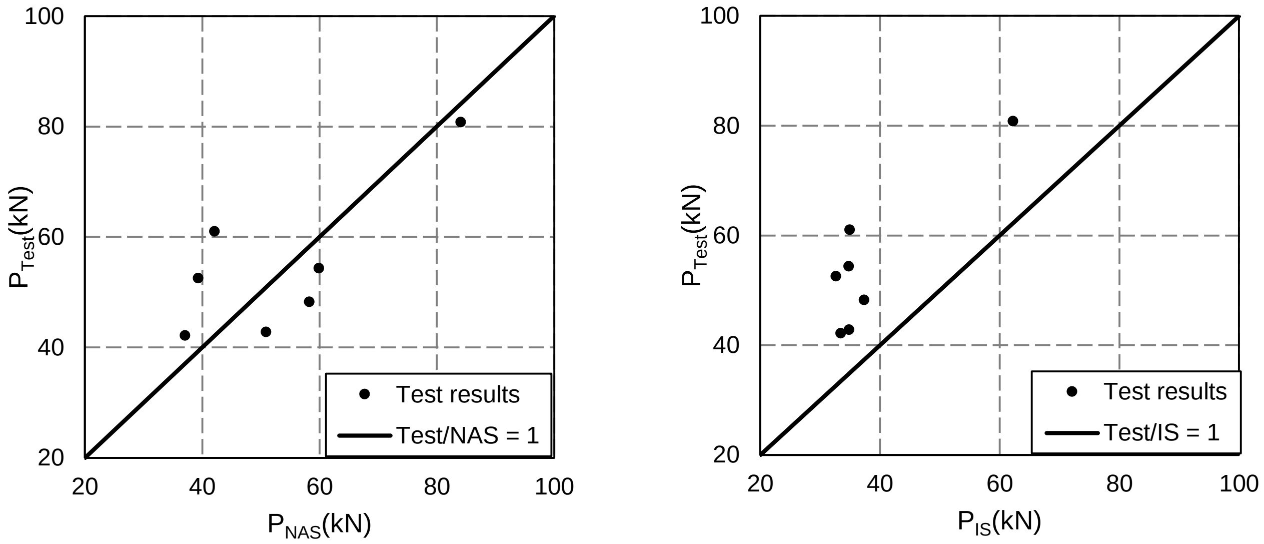

Fig. 18 Comparison of design strengths with the test results.

5. Conclusions

The experimental investigation of CFS built-up sections, with efficient intermediate stiffeners, subjected to bending has been presented. Simply supported beams were tested for major axis bending with two concentrated loads near the centre of the beam. The load-carrying capacity and failure modes of the beams were observed and reported. The experimental results were compared with predictions obtained from design standards. Based on this experimental study, the following conclusions are drawn:

- The provision of folds (intermediate stiffening) in open beam sections stimulates the outward movement of flanges and leads to distortion of the cross-section, thereby restricting its potential load-carrying capacity. However, this restriction can be overcome by restraining the outward movement of flanges by modifying the section or any other external means.
- The distortion as envisaged in case of open sections is restricted by the flange to flange connection in built-up closed sections, mainly due to the closed section's inherent resistance towards the same. Provision of folds (intermediate stiffeners) at either connection between web and flange reduced the unsupported width of the web significantly and considerably delayed buckling of the sections.
- The closed sections provide a higher strength-to-weight ratio in comparison to open sections. Further, their better performance under eccentric loading (torsion) and improved aesthetics suggest the use of closed sections over open beam sections.
- Bearing failure, local web and flange buckling, lateral torsional buckling, and distortional buckling were the failure modes observed in open beam sections. Local web buckling, flange buckling, and distortional buckling were observed in closed beam sections. Furthermore, the insufficient screw connections of bearing stiffeners connected to the web results in local buckling in the bearing stiffener itself. Hence, they failed to perform their intended use.
- The design predictions for efficient intermediate stiffened CFS beams using Indian Standards for CFS structures are conservative as IS 801 still adopts working stress design methodology. Further, IS 801 does not account for check for distortional buckling, therefore, it needs revision especially for closed sections subjected to flexure.

The design strengths for efficient intermediate stiffened CFS beams determined by using North American Standards for CFS structures overestimates the load-carrying capacity of open sections and underestimates the capacity of closed sections. The conservativeness in the design strength prediction of closed sections may be primarily due to their larger torsional rigidity compared to the open sections. Furthermore, open sections are more susceptible to local and distortional buckling. It is concluded that method of joining the elements of a built-up section has a marked influence on the section's load-carrying capacity and as such, this provision should be incorporated in the design codes to predict the load-carrying capacity of built-up sections more accurately.

The authors are presently working on the numerical validation of the cross-sectional profiles studied in this paper in order to carry out extensive parametric studies. This will help in modifying the current design guidelines for reliable design strength predictions for such sections. It will further help in need-based optimizing of the cross-sections.

This study investigated the flexural behaviour of efficient intermediate stiffened CFS beams. Future research is needed to study the shear behaviour of such beams, by conducting three-point loading tests on the same. However, adequate measures should be taken to prevent local buckling, especially at loading point. Furthermore, the influence of type of connection and the spacing between the fasteners connecting the various elements of the built-up section needs to be evaluated.

References

Dar, M.A., Sahoo, D.R. and Jain, A.K. (2019a), "Axial compression behavior of laced cold-formed steel built-up columns with unstiffened angle sections", *J. Constr. Steel Res.*, **162**, DOI: 10.1016/j.jcsr.2019.105727.

Dar, M.A., Subramanian, N., Dar, A.R., Anbarasu, M., Lim, J.B. and Mir, A. (2019b), "Behaviour of partly stiffened cold-formed steel built-up beams:Experimental investigation and numerical validation", *Adv. Struct. Eng.*, **22**(1), 172-186. https://doi.org/10.1177/1369433218782767.

Dar, M.A., Subramanian, N., Dar, A.R., Majid, M., Haseeb, M. and Tahoor, M. (2019c), "Structural efficiency of various strengthening schemes for cold-formed steel beams: Effect of global imperfections", *Steel Compos. Struct.*, **30**(4), 393-403. https://doi.org/10.12989/scs.2019.30.4.393.

Dar, M.A., Subramanian, N., Rather, A.I., Dar, A., Lim, J.B.P., Anbarasu, M. and Roy, K. (2019d), "Effect of angle stiffeners on the flexural strength and stiffness of cold-formed steel beams", *Steel Compos. Struct.*, **33**(2), 225-243. https://doi.org/10.12989/scs.2019.33.2.225.

Dar, M.A., Subramanian, N., Dar, D.A., Dar, A.R., Anbarasu, M., Lim, J.B. and Mahajoubi, S. (2020), "Flexural strength of cold-formed steel built-up composite beams with rectangular compression flanges", *Steel Compos. Struct.*, **34**(2), 171-188. https://doi.org/10.12989/scs.2020.34.2.171.

Dar M.A., Sahoo D.R., Pulikkal S. and Jain A.K. (2018a), "Behavior of laced built-up cold-formed steel columns: Experimental investigation and numerical validation", *Thin-Wall. Struct.*, **132**, 398-409. https://doi.org/10.1016/j.tws.2018.09.012.

Dar, M. A., Subramanian, N., Dar, A.R., Anbarasu, M. and Lim, J.B.P. (2018b), "Structural performance of cold-formed steel composite beams", *Steel Compos. Struct.*, **27**(5), 545-554. https://doi.org/10.12989/scs.2018.27.5.545.

Dar, M.A., Subramanian, N., Dar, A.R. and Raju, J. (2017), "Rehabilitation of a distressed steel roof truss – A study", *Struct. Eng. Mech.*, **62**(5), 567-576. https://doi.org/10.12989/sem.2017.62.5.567.

Dar, M.A., Dar, A.R., Yusuf, M. and Raju, J. (2015a), "Experimental study on innovative cold-formed steel beams", *Steel Compos. Struct.*, **19**(6), 1599-1610. https://doi.org/10.12989/scs.2015.19.6.1599.

Dar, M.A., Subramanian, N., Anbarasu, M., Dar, A.R. and Raju, J. (2015b), "Experimental investigations on the structural behaviour of a distressed bridge", *Struct. Eng. Mech.*, **56**(4), 695-705. https://doi.org/10.12989/sem.2015.56.4.695.

Grenda M. and Paczos P. (2019), "Experimental and numerical study of local stability of non-standard thin-walled channel beams", *J. Theor. Appl. Mech.*, **57**(3), 549-562. DOI 10.15632/jtam-pl/109601.

Hancock, G. (2016), "Cold-formed steel structures: Research review 2013–2014", *Adv. Struct. Eng.*, **19**(3), 393-408. https://doi.org/10.1177/1369433216630145.

Hot rolled medium and high tensile structural steel - specification. (2011), New Delhi: Bureau of Indian Standards.

Indian Standard- Metallic Testing- Tensile Testing at Ambient Temperature. (2005, May), New Delhi 110002: Bureau of Indian Standards.

IS 801-Code of Practice for use of cold formed light gauge steel structural members in general building construction. (1975), New Delhi: Bureau of Indian Standards.

Kumar, N. and Sahoo, D.R. (2016), "Optimization of lip length and aspect ratio of thin channel sections under minor axes bending", *Thin-Wall. Struct.*, **100**, 158-169. https://doi.org/10.1016/j.tws.2015.12.015.

Laím, L., Rodrigues, J.P.C. and daSilva, L. (2013), "Experimental and numerical analysis on the structural behaviour of cold-formed steel beams", *Thin-Wall. Struct.*, **72**, 1-13. https://doi.org/10.1016/j.tws.2013.06.008.

Magnucki, K. and Paczos, P. (2009), "Theoretical shape optimization of cold-formed thin-walled channel beams with drop flanges in pure bending", *J. Constr. Steel Res.*, **65**, 1731-1737. https://doi.org/10.1016/j.jcsr.2009.03.010.

Magnucki, K., Paczos, P. and Kasprzak, J. (2010), "Elastic buckling of cold-formed thin-walled channel beams with drop flanges",: *J. Struct. Eng. - ASCE*, **136**(7), 886-896. https://doi.org/10.1061/(ASCE)ST.1943-541X.0000184.

Manikandan, P., Sukumar, S. and Balaji, T. (2014), "Effective shaping of cold-formed thin-walled built-up beams in pure bending", *Arabian J. Sci. Eng.*, **39**, 6043-6054. https://doi.org/10.1007/s13369-014-1261-x.

North American Specification for the design of cold formed steel Structural members. (2016), Americal Iron and Steel Institute.

Obst, M., Rodak, M. and Paczos, P. (2016), "Limit load of cold formed thin-walled nonstandard channel beams", *J. Theor. App. Mech.*, **54**(4), 1369-1377.

Paczos, P. and Wasilewicz, P. (2009), "Experimental investigations of buckling of lipped, cold-formed thin-walled beams with I – section", *Thin-Wall. Struct.*, **47**(11), 1354-1362. https://doi.org/10.1016/j.tws.2009.03.009.

Schafer, B. (2006), "Designing cold-formed steel using the direct strength method", *Proceedings of the 18th International Specialty Conference on Cold-Formed Steel Structures.* Orlando, Florida.

Schafer, B. (2008), "Review: The Direct Strength Method of cold-formed steel member design", *J. Constr. Steel Res.*, **64**, 766-778.

Schafer, B.W. (2011), "Cold-formed steel structures around the world – A review of recent advances in applications, analysis and design", *Steel Constr.*, **4**(3) 141-149. https://doi.org/10.1002/stco.201110019.

SudhirSastry, Y.B., Krishna, Y. and Budarapu Pattabhi, R. (2015), "Parametric studies on buckling of thin walled channel beams", *Comput. Mater. Sci.*, **96**, 416-424. https://doi.org/10.1016/j.commatsci.2014.07.058.

Trahair, N.S. and Papangelis, J.P. (2018), "Lateral-distortional buckling of beams with hollow flanges and folded plate webs". *Eng. Struct.*, **163**, 71-76. ttps://doi.org/10.1016/j.engstruct.2018.02.001.

Wang, L. and Young, B. (2014), "Design of cold-formed steel channels with stiffened webs subjected to bending", *Thin-Wall. Struct.*, **85**, 81-92. https://doi.org/10.1016/j.tws.2014.08.002.

Ye, J., Becquea, J., Hajirasoulihaa, I., Mohammad Mojtabaeia, S. and Lim, J.B.P. (2018), "Development of optimum cold-formed steel sections for maximum energy dissipation in uniaxial bending", *Eng. Struct.*, **161**, 55-67. https://doi.org/10.1016/j.engstruct.2018.01.070.

Ye, J., Hajirasouliha, I., Becque, J. and Pilakoutas, K. (2016), "Development of more efficient cold-formed steel channel sections in bending", *Thin-Wall. Struct.*, **101**, 1-13. https://doi.org/10.1016/j.tws.2015.12.021.

Yu, C. and Schafer, B. (2006), "Distortional Buckling tests on cold-formed steel beams", *J. Struct. Eng.*, **132**(4), 515-528. https://doi.org/10.1061/(ASCE)0733-9445(2006)132:4(515).

Yu, J., Becquea, J., Hajirasoulihaa, I., Mojtabaei, S.M. and Lim, J.B.P. (2018), "Development of optimum cold-formed steel sections for maximum energy dissipation in uniaxial bending", *Eng. Struct.*, **161**, 55-67.

CC